Published in final edited form as:

Nat Cell Biol. 2015 March ; 17(3): 241–250. doi:10.1038/ncb3106.

Developmental regulation of apical endocytosis controls epithelial patterning in vertebrate tubular organs

Alejo E. Rodríguez-Fraticelli[1], **Jennifer Bagwell**[2], **Minerva Bosch-Fortea**[1], **Gaelle Boncompain**[3], **Natalia Reglero-Real**[5], **Maria J. García-León**[5], **Germán Andrés**[4], **Maria L. Toribio**[5], **Miguel A. Alonso**[5], **Jaime Millán**[5], **Franck Perez**[3], **Michel Bagnat**[2,*], and **Fernando Martín-Belmonte**[1,†]

[1]Dept. of Development and Differentiation, Centro de Biología Molecular “Severo Ochoa”, CSIC-UAM, Madrid, 28049, SPAIN

[2]Dept. of Cell Biology, Duke University, Durham , NC 27710, US

[3]Dept. of Subcellular Structure and Cellular Dynamics, UMR144, Institut Curie, Paris, 75005, FRANCE

[4]Electron Microscopy Core, Centro de Biología Molecular “Severo Ochoa”, CSIC-UAM, Madrid, 28049, SPAIN

[5]Dept. of Immunology and Cell Biology, Centro de Biología Molecular “Severo Ochoa”, CSIC-UAM, Madrid, 28049, SPAIN

Summary

Epithelial organs develop through tightly coordinated events of cell proliferation and differentiation in which endocytosis plays a major role. Despite recent advances, how endocytosis regulates development of vertebrate organs is still unknown. Here we describe a mechanism that facilitates the apical availability of endosomal SNARE receptors for epithelial morphogenesis through the developmental upregulation of Plasmolipin (*pllp*) in a highly endocytic segment of the zebrafish posterior midgut. PLLP recruits clathrin-adaptor EpsinR to sort the SNARE machinery of the endolysosomal pathway into the subapical compartment, which is a switch for polarized endocytosis. Furthermore, PLLP expression induces apical Crumbs (Crb) internalization and the activation of the Notch signaling pathway, both crucial steps in the acquisition of cell polarity and differentiation of epithelial cells. We thus postulate that differential apical endosomal SNARE sorting is a mechanism that regulates epithelial patterning.

[†]Correspondence: fmartin@cbm.csic.es. [*] m.bagnat@cellbio.duke.edu.

Author contributions

A.R-F., M.Ba. and F.M-B. designed the experiments; A.R-F, J.B., M.B-F. and G.A. carried out the experiments; A.R-F. and F.M-B. wrote the manuscript; G.B. and F.P. designed and constructed RUSH experimental tools; M.J.G-L. and M.L.T. designed and constructed the Notch-ligand tools; N.R., M.A., and J.M. produced and characterized the mammalian PLLP antibody; A.R-F. and G.A. designed and carried out the EM experiments.

Competing financial interests

The authors declare no competing financial interests.

Introduction

In order to establish functional barriers, epithelial cells require the formation of polarized protein transport machineriesn[1]. Endocytosis is one of such processes that become highly polarized[2]. Interestingly, recent studies have described that immature epithelial sheets have a reduced rate of apical endocytosis that intensifies along development[3], which suggests that epithelial cells acquire the ability to internalize material specifically from the apical pole during differentiation. Indeed, apical protein endocytosis regulates polarity and proliferation in Drosophila epithelial cells[4,5]. These findings suggest that endocytosis could be regulated during development to coordinate epithelial morphogenesis[6]. However, the molecular mechanisms of this endocytic regulation in epithelial organ development have not been previously characterized. To unveil developmentally regulated proteins that may control the process of apical endocytosis we used the zebrafish gut morphogenesis model[7,8]. We describe the role of the protein Plasmolipin (Pllp), which is induced in the posterior segment of the zebrafish intestine during morphogenesis, and is required for the generation of a highly endocytic enterocyte population during gut differentiation. We also characterize the molecular mechanism controlling PLLP function during endocytosis using the 3D-MDCK model. Using proteomics, we found that in 3D-MDCK cells PLLP interacts with EpsinR (EpsR), an AP1B-binding clathrin adaptor, which regulates the recycling of the endosomal SNAREs. Together, PLLP and EpsR are required for the sorting of endosomal SNAREs into the apical recycling compartment to properly feed the endocytic uptake of apical cargo. Finally, we demonstrate that the endocytic role of PLLP is essential for Crb downmodulation and Notch activation to promote absorptive cell differentiation.

Results

Plasmolipin (Pllp), is induced during epithelial tube formation in zebrafish and localizes to a highly endocytic compartment of the midgut

Gut morphogenesis is a genetically regulated process. To unveil genes developmentally controlled during epithelial gut morphogenesis we used a screen strategy based on the isolation of epithelial cells from the zebrafish gut[8]. We identified Plasmolipin (*pllp*) as one of the genes specifically induced during lumen formation and expansion (Figure 1A). Pllp is a type III-transmembrane protein of unknown function that belongs to the family of MARVEL-domain containing proteins associated with vesicle trafficking and membrane fusion[9]. We corroborated the expression of *pllp* in the gut using RNA *in situ* hybridization (ISH) (Figure 1B and Supplementary figure 1A). *pllp* is expressed in the hatching gland and the pronephric duct as early as 48hpf, and is highly enriched in the gut at 72 hpf and 120 hpf (Figure 1B, arrows, and Supplementary figure 1A). To analyze the subcellular localization of the Pllp protein, we used BAC recombineering[10] to generate a bacterial artificial chromosome (BAC) expressing Pllp-GFP and obtained stable transgenic animals *TgBAC(pllp-spGFP)*. We found that Pllp expression is highly induced in a specific segment of the posterior midgut (PGS) at 120 hpf (Figure 1C and Supplementary figure 1B). Pllp-GFP localizes to the apical region of intestinal epithelial cells (IECs), with a small population associated with internal membranes (Figure 1D, arrowheads, and Supplementary figure 1C). To further evaluate the subcellular localization of the protein, we performed anti-

GFP immunogold electron microscopy (EM) in gut sections (Figure 1E). The majority of Pllp-GFP (65%) localized to small tubules and vesicles (about 70-100 nm wide) present in the first 300 nm below the apical membrane, with a small fraction of PLLP also distributed both to the apical microvilli and more basal endosomes. This polarized localization of Pllp suggests a function associated with the apical endocytic pathway.

Therefore, we next analyzed if Pllp is involved in apical endocytosis in the zebrafish gut by using microgavaging to deliver endocytic tracers directly into the intestinal lumen[11] (Figure 1F). Interestingly, gavaged Dextran-TR was specifically internalized in the posterior midgut in 144 hpf *TgBAC(pllp-spGFP)* larvae where Pllp is enriched (Figure 1G, arrows). Furthermore, we observed that Lamp2, a late endosomal marker, is specifically enriched in Pllp-positive cells (Figure 1H, arrows). Thus Pllp is a marker of highly endocytic enterocytes of the posterior midgut at the onset of intestinal differentiation.

Pllp is required for apical endocytosis and endosomal maturation in the zebrafish posterior midgut

To analyze if Pllp is required for apical endocytosis in the gut, we generated a mutant allele using TAL-effector nucleases (TALENs)[12]. We identified one allele that contained an insertion/deletion (*pd1116*), giving rise to a frame-shift mutation and an early STOP codon, which truncates 85% of the protein structure (Supplementary figure 1D). Homozygous *pllp*^{pd1116} larvae develop normal early gut morphology and intestinal cell numbers (Supplementary figure 1E-F), but present marked defects in the number of endocytic cells and the amount of dextran that was internalized in the PGS (Figure 2A-B). In addition, at 144 hpf, *pllp*^{pd1116} IECs are significantly shorter than WT (Figure 2C and Supplementary figure 1G), a phenotype also observed in *pllp* morphants (Supplementary figure 1H-J), and present stubbier microvilli (Supplementary figure 1K). To more precisely evaluate the internalization defects, we gavaged *pllp*^{pd1116} larvae with Dextran-TR and BSA-conjugated 15 nm gold for ultrastructural analysis. IECs of *pllp*^{pd1116} larvae present alterations in apical endosome numbers and size distribution, and negligible levels of apical BSA-gold endocytosis compared to WT (Figure 2D, Supplementary figure 1G, arrows, and Supplementary figure 1L). At later time points, juvenile *pllp*^{pd1116} mutants (75%) present disrupted intestinal folds and a 1.4-fold expansion in apical membrane size (Figure 2E and Supplementary figure 1M), a phenotype resembling previous observations in *Drosophila* mutants with disrupted apical endocytosis[5]. The survival of *pllp*^{pd1116} mutants raised with a limited food supply was highly compromised compared to WT juveniles, suggesting that Pllp is necessary for efficient nutrient absorption (Supplementary figure 1N). We validated the specificity of phenotypes by crossing *pllp*^{pd1116} mutants to *TgBAC(pllp-GFP)* heterozygous animals. Pllp-GFP expression almost completely rescued both the endocytic and the cell-height phenotypes of the *pllp*^{pd1116} mutation, indicating that the lack of *pllp* expression in the mutants is the specific cause of the observed defects in IECs and that the fusion protein is functional (Supplementary figure 1O-P). To summarize, these results indicate that Pllp is required for apical endocytosis and epithelial morphogenesis in the gut and suggest a function in regulating terminal epithelial differentiation of posterior gut enterocytes.

PLLP regulates formation of apical recycling endosomes

The subapical localization of PLLP suggests its association with apical recycling endosomes (ARE), which are required for the recycling of endocytosed receptors back to the plasma membrane[13]. Endogenous Rab11, an ARE marker, partially colocalized with subapical Pllp (Figure 2F, arrows, r=0.64±0.09). We observed that in *pllp*^{pd1116} mutants Rab11 is mislocalized throughout the cytoplasm in posterior gut IECs, before any morphogenetic defects arise (Figure 2G-H and Supplementary figure 1Q), suggesting that Pllp is required for the formation or maintenance of a polarized ARE compartment, and possibly for protein recycling at the onset of epithelial morphogenesis. In addition, EM images of IECs revealed that *pllp*^{pd1116} mutants presented a 2.6-fold decrease in the number of recycling/sorting tubules in apical endosomes compared to WT (Figure 2D, inserts, 2I and Supplementary figure 2A). In conclusion, Pllp is required for polarized Rab11 distribution in epithelial cells, suggesting that Pllp is required for the formation or maintenance of the ARE compartment, and possibly for protein recycling from apical sorting endosomes during epithelial morphogenesis.

PLLP is required for epithelial morphogenesis and endosomal maturation in MDCK cysts

To dissect more precisely the molecular function of PLLP we used the 3D-MDCK model system, which aptly recapitulates epithelial morphogenesis *in vitro*[14]. PLLP expression increases during lumen formation and localizes to the subapical compartment in 3D-MDCK cells (Figure 3A-B). We also observed a similar pattern of expression in sections of mouse small intestine and kidney (Supplementary figure 2B-C), mimicking the subcellular localization and expression patterns observed in zebrafish. This common pattern of subcellular localization in epithelial tubes suggests a potential similar role in all these tissues. Consistently, silencing of PLLP (PLLP-KD) results in morphogenetic defects (Figure 3C-E and Supplementary figure 2D-E) and endolysosomal function defects (Figure 2F-G). Furthermore, PLLP also partially colocalizes with Rab11 (r=0.73±0.12) and PLLP-KD disrupts ARE polarization (Supplementary figure 2F-G). These results suggest a conserved role for PLLP in ARE polarization and endosomal maturation. Next, we tested if PLLP overexpression is sufficient to enhance formation of Rab11 endosomes. Overexpression of PLLP-GFP in monolayers of MDCK cells (2D) induces the formation of an enlarged Rab11-positive compartment, which colocalizes with early endosomal markers and induces the formation of acidic endosomes (Figure 3H). This PLLP-GFP compartment consisted of clusters of vesicles that resembled ARE tubule-vesicles (Supplementary figure 2H). *TgBAC(pllp-GFP)pd1114* line, which overexpresses Pllp-GFP, presents a similar phenotype (Supplementary figure 2I). In summary, these experiments indicate that PLLP is required for endosomal maturation and ARE polarization, and furthermore that PLLP expression is sufficient to expand the ARE, and enhance formation of lytic acidic endosomes.

PLLP interacts with EpsR to sort endosomal SNAREs to the recycling compartment

To characterize the molecular mechanism associated with PLLP function, we devised an *in vivo* biotinylation assay (bioID) of PLLP-proximal proteins (Figure 4A). We uncovered 42 proteins likely to interact with PLLP in 3D-MDCK cells, including 20 proteins with

trafficking functions and 9 SNARE proteins or SNARE regulators (Supplementary table 1 and 2). We identified Clint-1/Epsin-4/EpsR (hereafter termed EpsR) as the principal interacting partner of PLLP (Figure 4B). EpsR belongs to the Epsin family of membrane tubulating proteins and it is required for retrograde transport from late endosomes[15-17]. The N-terminal ENTH domain of EpsR has been described to interact with several cargoes, including endosomal SNAREs, and is required for SNARE recycling[18-20]. We confirmed the interaction between endogenous PLLP and the C-terminal domain of EpsR (Figure 4C) and found that EpsR and PLLP partially co-localize in internal endosomes (Figure 4D, arrows, and Supplementary figure 3A, arrows, r=0.61±0.08). PLLP-KD cells present a dispersed and decreased staining of both EpsR and Rab7 (Figure 4E and Supplementary figure 3B) suggesting that PLLP is required for EpsR endosomal localization and maturation of degradative endosomes. EpsR silencing phenocopies PLLP-KD (Figure 4F, 4L, and Supplementary figure 3C-D) and inhibits PLLP gain-of-function phenotypes (Supplementary figure 3E), indicating that EpsR binding to PLLP is required for the formation of apical Rab11-positive endosomes. Interestingly, the *Drosophila* EpsR homolog, *Liquid-facets related* (*lqfR*) is a regulator of epithelial cell morphology and regulates cell height in the follicle cells of the egg-chamber[21,22], which, together with our results, suggests EpsR function in epithelial morphogenesis is conserved across bilateria.

Next, we investigated one of the canonical cargoes of EpsR, Syntaxin-7 (Stx7) (Miller et al., 2007), which was also identified in our bioID assay (Supplementary table 2). Stx7 is highly polarized to the subapical endosomal compartment in 3D-MDCK (Figure 4G) and mouse intestine (Supplementary figure 3F). Furthermore Stx7 and PLLP colocalize in the subapical compartment (Figure 4G, arrowheads, r=0.83±0.05), and interact in these membrane domains as we observed using a probe-ligation assay (PLA)(Supplementary figure 3G-H)[23]. Next, we addressed if Stx7 subapical localization requires PLLP and EpsR. We found that silencing either PLLP or EpsR mislocalized Stx7 from the subapical compartment (Figure 4G-H). FRAP analysis of subapical endosomes revealed similar recovery kinetics for both proteins (k_{off} Stx7, 0.022 s^{-1}; k_{off} PLLP, 0.026 s^{-1}), suggesting that they traffic in the same carriers to the subapical compartment (Figure 4I-J, Video 1). Moreover, we found that Stx7 silencing phenocopies PLLP and EpsR-KD (Figure 4K-L and Supplementary figure 3I-L). Consistently, *pllp*^{pd1116} larvae showed a scattered distribution of Stx7, recapitulating PLLP-KD in MDCK cysts (Supplementary figure 3M).

Together these results indicate that endosomal SNAREs are polarized in the subapical compartment in epithelial cells and recycled back to the apical pole from sorting/late endosomes by interacting with PLLP and EpsR. These data also imply that formation of Rab11 endosomes depends on the maintenance of apical endosomal fusion and a cyclic dependence of both apical endocytosis and the recycling of the SNARE fusion machinery.

PLLP regulates Crb endocytosis and Notch signaling during epithelial morphogenesis

Our data suggest the possibility that PLLP levels could modulate endocytosis and degradation of apical protein receptors. Crb is a master regulator of epithelial morphogenesis and is regulated by endocytosis[24-26]. *In vivo*, *pllp*^{pd1116} mutants displayed higher levels of Crumbs (Figure 5A-B). In 3D-MDCK cells, Crumbs3 (Crb3) becomes progressively

restricted to tight junctions (TJ) (Figure 5C and Supplementary figure 4A), correlating with the timing of PLLP induction, whereas PLLP-KD cells present Crb3 mislocalized to the apical plasma membrane and higher total levels of Crb3 (Figure 5D and 5E, arrowheads, and Supplementary figure 4A-C). Crb3 missorting could be explained by a defect in protein sorting to the TJ or by a defect in endocytosis at the apical plasma membrane. To dynamically address GFP-Crb3(a) localization we used the RUSH system (Supplementary video 2)[27]. GFP-Crb3 is secreted first at the apical plasma membrane from where it then relocalizes to the TJ (Figure 5F, top panels, arrows, and Supplementary video 3). PLLP-KD or endocytosis inhibitor-treated 3D-MDCK cells fail to segregate Crb3 later to the TJ (Figure 5F, middle and bottom panels, Supplementary video 4 and 5). Moreover, PLLP overexpression is sufficient to induce Crb3 endocytosis and downmodulation (Figure 5G-I). Our results suggest that PLLP expression is necessary and sufficient to control Crb3 levels directly through regulation of apical endocytosis.

Notch signaling is required for absorptive intestinal cell differentiation across evolution[25,28,29] and the Stx7 homolog, *avl*, is required for Notch signaling in *Drosophila*[30]. PLLP-KD or EpsR-KD reduces activated Notch (NICD) levels by 60 and 40% respectively (Figure 6A) and PLLP-KD inhibits full-length Notch1a localization in endosomes (Figure 6B, arrows), whereas the overexpression of PLLP-GFP is sufficient to induce Notch1a internalization. These results suggested that PLLP is required for Notch-receptor endocytosis and activation. However, Notch activation also requires Epsin-mediated endocytosis of Notch ligands[31,32]. To further analyze whether PLLP and EpsR are required for receptor or ligand activation, we cultured Notch1a-expressing MDCK cells over mesenchymal OP9 cell layers stably expressing Jagged-1 or Delta-like 1, the main ligands expressed in the zebrafish gut[33]. PLLP-KD and EpsR-KD inhibited Notch1 transactivation specifically by Jagged-1, and not by Delta-like1 (Figure 6C-E and Supplementary figure 4D). Then, we co-cultured Notch1-expressing MDCK cells with Jagged-1-MDCK cells, and confirmed that Notch-receptor cells require the expression of both PLLP and EpsR, whereas EpsR expression appears to be also required in the ligand-presenting cells (Supplementary figure 4E-H). These results indicate that PLLP is induced in Notch-receptor cells to specifically regulate Notch activity in these cells.

Next, we analyzed Notch signaling *in vivo*. The *pllp*^{pd1116} mutants present a reduced number of terminally differentiated vacuolated cells and a three-fold increase of PAS-positive mucosecretory cells (Figure 6F-G). Moreover, *pllp*^{pd1116} mutants show a marked decrease in expression of *bona fide* Notch-effector gene Her15 (Figure 6H), similarly to what has been previously reported for Mindbomb (*mib*) mutations, in which Jagged/Serrate-family ligands are unable to signal to Notch-positive cells[33]. Altogether, these results indicate that Pllp is required for Notch signaling, terminal differentiation of posterior gut enterocytes and inhibition of secretory cell differentiation in the posterior midgut. To analyze if Notch signaling is required for terminal differentiation of the posterior vacuolated IECs, we gavaged 144hpf Mindbomb *mib1*^{ta52b} mutant larvae and Notch inhibitor-treated larvae. Both exhibited a significant reduction in the number of endocytic cells and the size of endosomes (Figure 6I, arrows). Altogether, these experiments indicate that Pllp controls Notch activity, which is essential for absorptive enterocyte terminal differentiation in the posterior midgut.

Discussion

Here, we characterized a developmentally regulated mechanism to induce apical endocytosis through the regulation of SNARE sorting which is necessary for epithelial morphogenesis (Figure 6J). We propose that endosomal SNAREs are polarized to different endosomal networks at the apical and basolateral domains. Apical SNARE sorting is controlled to regulate the rate of apical protein endocytosis, involved in receptor degradation and signaling. We describe that expression of a previously uncharacterized protein, PLLP, induces SNARE recycling through its interaction with the membrane tubulating clathrin adaptor EpsR (Figure 6J).

Additionally, our experiments demonstrate that PLLP is induced in a time and space-specific manner to regulate the *in vivo* differentiation of a notch-mediated highly-endocytic absorptive cell population in the zebrafish midgut (Figure 6J). Epithelial morphogenesis is a finely regulated process in which epithelial cells conduct a delicate balancing act between differentiation and proliferation that becomes deregulated in different types of human carcinomas[34]. Epithelial cell differentiation greatly depends on the establishment of cellular junctions and polarity complexes that serve to organize the physiology of mature epithelial tissues. These polarity complexes, such as the Crb complex, crosstalk with proliferation pathways, such as the Notch pathway, in order to prevent overgrowth and, at the same time, to provide a functional population of highly differentiated epithelial cells[4]. Our experiments indicate that PLLP fine-tunes Notch signaling for differentiation of posterior gut absorptive cells. Adult *pllp* mutants presented posterior guts that resembled more anterior compartments, with a reduced population of vacuolated cells and increased populations of mucosecretory cells (Figure 6J).

Pllp is also expressed in several other epithelial-like cell types in zebrafish not described here, such as a subpopulation of skin cells, the sheath cells of the notochord, and the neuromasts of the lateral line. Interestingly, asymmetric proliferation and differentiation of these cell types also depend on Notch signaling[35-37]. Further studies will be directed to understanding the role of PLLP in fine-tuning Notch activity during development of these organs.

Supplementary Material

Refer to Web version on PubMed Central for supplementary material.

Acknowledgements

We thank Carmen M. Ruiz-Jarabo for her comments on the manuscript and members of the Martin-Belmonte lab and Bagnat labs for helpful discussions. We thank Ashley Alvers (Duke University, NC, USA) for helping in the isolation of gut cells, Jordan Cocchiaro and Lindsey Marjoram (Duke University, NC, USA) for help in gavaging experiments, Ben Margolis (University of Michigan, MI, USA) for the Crb3/pan-Crb antibody, Reinhardt Jahn (Max Planck Institute for Biophysical Chemistry, Germany) for Stx7 plasmids, Margaret Robinson (University of Cambridge, United Kingdom) for EpsR plasmids, and Raphael Kopan and Jose Luis de la Pompa (CNIC, Spain) for Notch plasmids and *mib1*^{ta52b} embryos. We also thank M. Guerra at the EM Unit for skillful technical assistance. This work was supported by grants from the MINECO (BFU2011-22622) and CONSOLIDER (CSD2009-00016) to F.M-B, by grant SAF2013-44857-R to MLT, by NIH innovator grant 1DP2OD006486 to M.Ba, and by grant AGL2013-48998-C2-2-R to G.A. A.E.R-F was supported by a CSIC JAE PhD fellowship. M.B-F is a recipient of a

Fundación Obra Social “La Caixa” PhD fellowship. G.A. was supported by the Amarouto Program for senior researchers from the Comunidad Autónoma de Madrid.

REFERENCES

1. Rodriguez-Boulan E, Macara IG. Organization and execution of the epithelial polarity programme. Nature reviews. Molecular cell biology. 2014; 15:225–242. doi:10.1038/nrm3775. [PubMed: 24651541]
2. Eaton S, Martin-Belmonte F. Cargo Sorting in the Endocytic Pathway: A Key Regulator of Cell Polarity and Tissue Dynamics. Cold Spring Harbor perspectives in biology. 2014 doi:doi: 10.1101/cshperspect.a016899.
3. Fabrowski P, et al. Tubular endocytosis drives remodelling of the apical surface during epithelial morphogenesis in Drosophila. Nature communications. 2013; 4:2244. doi:10.1038/ncomms3244.
4. Richardson EC, Pichaud F. Crumbs is required to achieve proper organ size control during Drosophila head development. Development. 2010; 137:641–650. doi:10.1242/dev.041913. [PubMed: 20110329]
5. Lu H, Bilder D. Endocytic control of epithelial polarity and proliferation in Drosophila. Nature cell biology. 2005; 7:1232–1239. doi:10.1038/ncb1324. [PubMed: 16258546]
6. Bokel C, Brand M. Endocytosis and Signaling during Development. Cold Spring Harbor perspectives in biology. 2014; 6 doi:10.1101/cshperspect.a017020.
7. Bagnat M, Cheung ID, Mostov KE, Stainier DY. Genetic control of single lumen formation in the zebrafish gut. Nature cell biology. 2007; 9:954–960. doi:10.1038/ncb1621. [PubMed: 17632505]
8. Alvers AL, Ryan S, Scherz PJ, Huisken J, Bagnat M. Single continuous lumen formation in the zebrafish gut is mediated by smoothened-dependent tissue remodeling. Development. 2014; 141:1110–1119. doi:10.1242/dev.100313. [PubMed: 24504339]
9. Sanchez-Pulido L, Martin-Belmonte F, Valencia A, Alonso MA. MARVEL: a conserved domain involved in membrane apposition events. Trends in biochemical sciences. 2002; 27:599–601. [PubMed: 12468223]
10. Navis A, Marjoram L, Bagnat M. Cftr controls lumen expansion and function of Kupffer's vesicle in zebrafish. Development. 2013; 140:1703–1712. doi:10.1242/dev.091819. [PubMed: 23487313]
11. Cocchiaro JL, Rawls JF. Microgavage of zebrafish larvae. Journal of visualized experiments : JoVE. 2013:e4434. doi:10.3791/4434. [PubMed: 23463135]
12. Cermak T, et al. Efficient design and assembly of custom TALEN and other TAL effector-based constructs for DNA targeting. Nucleic acids research. 2011; 39:e82. doi:10.1093/nar/gkr218. [PubMed: 21493687]
13. Golachowska MR, Hoekstra D, van ISC. Recycling endosomes in apical plasma membrane domain formation and epithelial cell polarity. Trends in cell biology. 2010; 20:618–626. doi:10.1016/j.tcb.2010.08.004. [PubMed: 20833047]
14. Galvez-Santisteban M, et al. Synaptotagmin-like proteins control the formation of a single apical membrane domain in epithelial cells. Nature cell biology. 2012; 14:838–849. doi:10.1038/ncb2541. [PubMed: 22820376]
15. Saint-Pol A, et al. Clathrin adaptor epsinR is required for retrograde sorting on early endosomal membranes. Developmental cell. 2004; 6:525–538. [PubMed: 15068792]
16. Mills IG, et al. EpsinR: an AP1/clathrin interacting protein involved in vesicle trafficking. The Journal of cell biology. 2003; 160:213–222. doi:10.1083/jcb.200208023. [PubMed: 12538641]
17. Hirst J, Motley A, Harasaki K, Peak Chew SY, Robinson MS. EpsinR: an ENTH domain-containing protein that interacts with AP-1. Molecular biology of the cell. 2003; 14:625–641. doi:10.1091/mbc.E02-09-0552. [PubMed: 12589059]
18. Miller SE, Collins BM, McCoy AJ, Robinson MS, Owen DJ. A SNARE-adaptor interaction is a new mode of cargo recognition in clathrin-coated vesicles. Nature. 2007; 450:570–574. doi:10.1038/nature06353. [PubMed: 18033301]
19. Chidambaram S, Zimmermann J, von Mollard GF. ENTH domain proteins are cargo adaptors for multiple SNARE proteins at the TGN endosome. Journal of cell science. 2008; 121:329–338. doi:10.1242/jcs.012708. [PubMed: 18198191]

20. Chidambaram S, Mullers N, Wiederhold K, Haucke V, von Mollard GF. Specific interaction between SNAREs and epsin N-terminal homology (ENTH) domains of epsin-related proteins in trans-Golgi network to endosome transport. The Journal of biological chemistry. 2004; 279:4175–4179. doi:10.1074/jbc.M308667200. [PubMed: 14630930]
21. Leventis PA, et al. Liquid facets-related (lqfR) is required for egg chamber morphogenesis during Drosophila oogenesis. PloS one. 2011; 6:e25466. doi:10.1371/journal.pone.0025466. [PubMed: 22043285]
22. Zhou D, et al. Mst1 and Mst2 maintain hepatocyte quiescence and suppress hepatocellular carcinoma development through inactivation of the Yap1 oncogene. Cancer cell. 2009; 16:425–438. doi:10.1016/j.ccr.2009.09.026. [PubMed: 19878874]
23. Leuchowius KJ, Weibrecht I, Soderberg O. Robinson, J. PaulIn situ proximity ligation assay for microscopy and flow cytometry. Current protocols in cytometry. 2011 Chapter 9, Unit 9 36, doi: 10.1002/0471142956.cy0936s56.
24. Thompson BJ, Pichaud F, Roper K. Sticking together the Crumbs - an unexpected function for an old friend. Nature reviews. Molecular cell biology. 2013; 14:307–314. doi:10.1038/nrm3568.
25. Fre S, Bardin A, Robine S, Louvard D. Notch signaling in intestinal homeostasis across species: the cases of Drosophila, Zebrafish and the mouse. Experimental cell research. 2011; 317:2740–2747. doi:10.1016/j.yexcr.2011.06.012. [PubMed: 21745469]
26. Harder JL, Whiteman EL, Pieczynski JN, Liu CJ, Margolis B. Snail destabilizes cell surface Crumbs3a. Traffic. 2012; 13:1170–1185. doi:10.1111/j.1600-0854.2012.01376.x. [PubMed: 22554228]
27. Boncompain G, et al. Synchronization of secretory protein traffic in populations of cells. Nature methods. 2012; 9:493–498. doi:10.1038/nmeth.1928. [PubMed: 22406856]
28. VanDussen KL, et al. Notch signaling modulates proliferation and differentiation of intestinal crypt base columnar stem cells. Development. 2012; 139:488–497. doi:10.1242/dev.070763. [PubMed: 22190634]
29. van Es JH, et al. Notch/gamma-secretase inhibition turns proliferative cells in intestinal crypts and adenomas into goblet cells. Nature. 2005; 435:959–963. doi:10.1038/nature03659. [PubMed: 15959515]
30. Vaccari T, Lu H, Kanwar R, Fortini ME, Bilder D. Endosomal entry regulates Notch receptor activation in Drosophila melanogaster. The Journal of cell biology. 2008; 180:755–762. doi: 10.1083/jcb.200708127. [PubMed: 18299346]
31. Wang W, Struhl G. Distinct roles for Mind bomb, Neuralized and Epsin in mediating DSL endocytosis and signaling in Drosophila. Development. 2005; 132:2883–2894. doi:10.1242/dev.01860. [PubMed: 15930117]
32. Wang W, Struhl G. Drosophila Epsin mediates a select endocytic pathway that DSL ligands must enter to activate Notch. Development. 2004; 131:5367–5380. doi:10.1242/dev.01413. [PubMed: 15469974]
33. Crosnier C, et al. Delta-Notch signalling controls commitment to a secretory fate in the zebrafish intestine. Development. 2005; 132:1093–1104. doi:10.1242/dev.01644. [PubMed: 15689380]
34. Martin-Belmonte F, Perez-Moreno M. Epithelial cell polarity, stem cells and cancer. Nature reviews. Cancer. 2012; 12:23–38. doi:10.1038/nrc3169.
35. Yamamoto M, et al. Mib-Jag1-Notch signalling regulates patterning and structural roles of the notochord by controlling cell-fate decisions. Development. 2010; 137:2527–2537. doi:10.1242/dev.051011. [PubMed: 20573700]
36. Wibowo I, Pinto-Teixeira F, Satou C, Higashijima S, Lopez-Schier H. Compartmentalized Notch signaling sustains epithelial mirror symmetry. Development. 2011; 138:1143–1152. doi:10.1242/dev.060566. [PubMed: 21343366]
37. Liu Y, Pathak N, Kramer-Zucker A, Drummond IA. Notch signaling controls the differentiation of transporting epithelia and multiciliated cells in the zebrafish pronephros. Development. 2007; 134:1111–1122. doi:10.1242/dev.02806. [PubMed: 17287248]
38. Bosse F, Hasse B, Pippirs U, Greiner-Petter R, Muller HW. Proteolipid plasmolipin: localization in polarized cells, regulated expression and lipid raft association in CNS and PNS myelin. Journal of neurochemistry. 2003; 86:508–518. [PubMed: 12871592]

39. Schier AF, et al. Mutations affecting the development of the embryonic zebrafish brain. Development. 1996; 123:165–178. [PubMed: 9007238]

40. Doyle EL, et al. TAL Effector-Nucleotide Targeter (TALE-NT) 2.0: tools for TAL effector design and target prediction. Nucleic acids research. 2012; 40:W117–122. doi:10.1093/nar/gks608. [PubMed: 22693217]

41. Rodriguez-Fraticelli AE, et al. The Cdc42 GEF Intersectin 2 controls mitotic spindle orientation to form the lumen during epithelial morphogenesis. The Journal of cell biology. 2010; 189:725–738. doi:10.1083/jcb.201002047. [PubMed: 20479469]

42. Roux KJ, Kim DI, Raida M, Burke B. A promiscuous biotin ligase fusion protein identifies proximal and interacting proteins in mammalian cells. The Journal of cell biology. 2012; 196:801–810. doi:10.1083/jcb.201112098. [PubMed: 22412018]

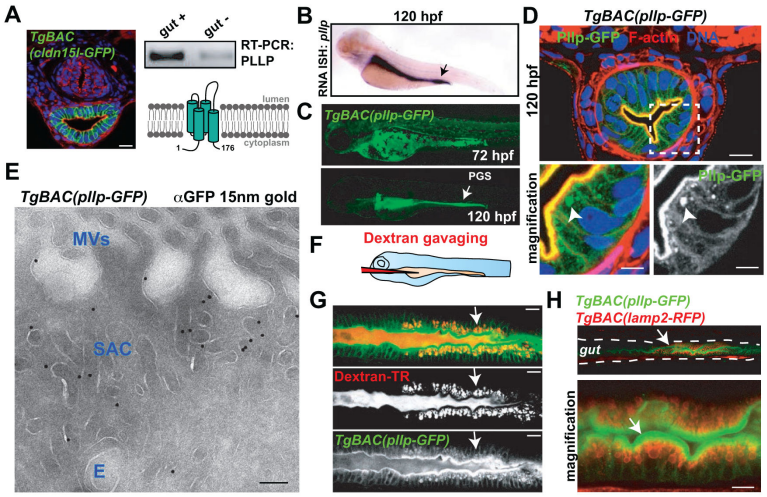

Figure 1. *pllp* expression is induced in endocytic enterocytes during development

(A) Identification of *pllp* as a gene induced during gut morphogenesis. Gut cells were FACS sorted from *TgBAC(cldn15la-GFP)* zebrafish larvae and gut-specific cDNAs were cloned by RT-PCR. Bottom right, scheme of predicted PLLP structure showing N and C-terminal cytoplasmic tails. Scale, 10 μm.

(B) In situ hybridization of *pllp* DIG-labeled RNA probe at 120hpf. Arrow indicates the gut.

(C) *TgBAC(pllp-GFP)* transgenic zebrafish larvae. A spacer-GFP sequence was recombined in place of the STOP codon using a zebrafish BAC clone carrying the full *pllp* gene. Notice the posterior midgut segment (PGS) contains a population of $PLLP^{high}$ cells (arrow).

(D) Transverse section of *TgBAC*(*pllp-GFP*) larva posterior midgut, stained using Phalloidin (which labels F-actin in apical microvilli, in red) and DAPI (for DNA, in blue). Arrowheads indicate apical endosomes. Scale, 10 μm (magnification, 5 μm)

(E) Immunogold electron microscopy of *TgBAC*(*pllp-GFP*) using anti-GFP and protein-A gold particles. The majority of labeled protein (65%) resides in a subapical endosomal compartment (SAC), whereas 15% of the label localized to microvilli (MVs) and 13% was labeling more basal localized endosomes (E). Scale, 100 nm.

(F) Gavaging of zebrafish larvae. Dextran-Texas Red was force-fed by microinjection into anesthetized 144hpf larvae.

(G) Dextran gavaged *TgBAC*(*pllp-GFP*) larvae. *TgBAC*(*pllp-GFP*) larvae were gavaged with dextran-TR and analyzed by live confocal microscopy 2h post-gavaging. Notice the dextran is endocytosed only in the posterior midgut (arrow), where Pllp expression is higher. Scale, 20 μm.

(H) *TgBAC(pllp-GFP)*;*TgBAC(lamp2-spRFP)* 144hpf larvae analyzed by live confocal microscopy. Lamp2 is localized specifically to the posterior midgut (arrows). Scale, 10 μm.

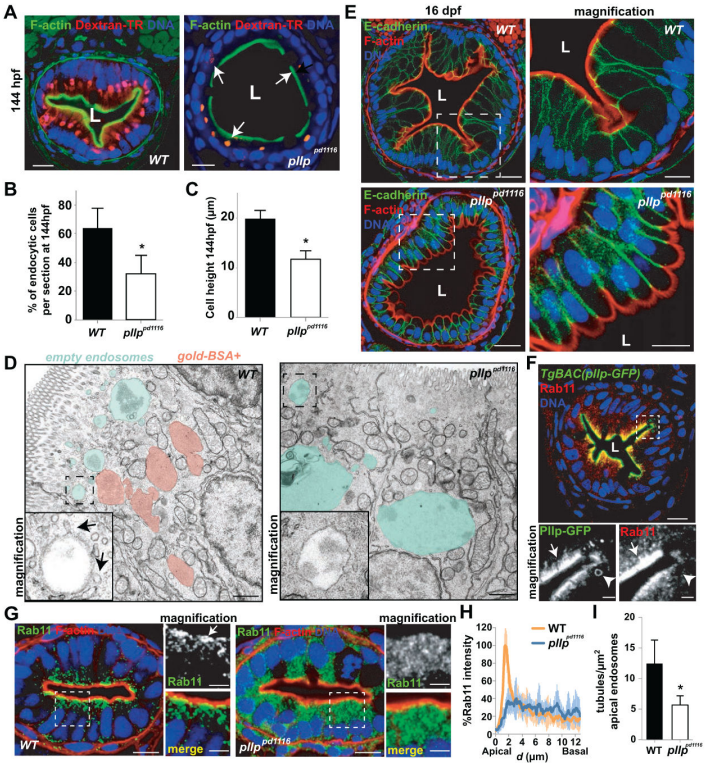

Figure 2. Pllp is required for apical endocytosis and epithelial morphogenesis in the zebrafish gut

(A) Endocytosis of dextran in *pllp*^{pd1116} mutants. Posterior midgut sections of dextran-gavaged (red) 144hpf larvae were labeled with Phalloidin (green) and DAPI (blue). Arrows indicate remaining cells that are able to endocytose dextran in the mutant. L, lumen. Scale, 10 µm.

(B) Quantification of endocytic cells in *pllp*^{pd1116} mutants. Data are mean±SD percentage of endocytic cells (WT, 63.9±8.2%; *pllp* ^{pd1116} 32±9,3%; n=10 sections from 5 wt and 6 mutant fish, randomly selected from 3 independent gavaging experiments; *p<0.005).

(C) Quantification of cell-height in *pllp*^{pd1116} mutants. Data are mean±SD cell height in µm (WT, 19.7±1.8 µm; *pllp*^{pd1116}, 11.7±1.7 µm; n=10 sections from 7 wt and 6 mutant fish, randomly selected from 3 independent experiments; *p<0.005).

(D) EM sections of *pllp*^{pd1116} mutant fish gavaged with dextran and BSA-gold(15nm). BSA-positive compartments (red) and BSA-empty endosomes (green) are colored. Scale, 1 µm.

(E) Epithelial morphology is disrupted in *pllp*^{pd1116} juveniles. Larvae were raised in 1L tanks, fixed at 16dpf, sectioned and stained with the anti-E-cadherin antibody (green), phalloidin (red) and DAPI (blue). L, lumen. Scale, 20 µm (magnification, 10 µm).

(F) PLLP and Rab11a colocalization in zebrafish enterocytes. *TgBAC(pllp-GFP)* 144hpf guts are labeled with anti-Rab11 (red) and DAPI (blue). Arrows indicate colocalization. Arrowheads indicate Rab11-negative PLLP endosomes. L, lumen. Scale, 10 µm (magnification, 5 µm).

(G) Rab11 localization in WT and *pllp*^{pd1116} 96hpf larval guts. Larvae were fixed, sectioned and stained with anti-Rab11 (green), Phalloidin (red) and DAPI (blue). Arrow indicates the subapical compartment. Scale, 10 µm (magnification, 5 µm).

(H) Quantification of Rab11 localization in (G). Fluorescent intensity linear profiles were drawn perpendicular to the center of the apical plasma membrane (0 is the peak of apical F-actin staining). Data are averaged linear profiles±SD (n=16 wt and 12 mutant cells from 3 independent experiments).

(I) Quantification of tubulating membranes in WT and *pllp*^{pd1116} larvae. The number of connected tubular structures was counted in every apical endosome (>300 nm diameter). For every endosome, the endosomal surface was determined as a function of perimeter × slice depth. Results are represented as number of tubules counted per endosomal surface unit (in μm^2)±SD (n = 5 wt and 5 mutant fish pooled from 2 independent experiments; *p<0.05).

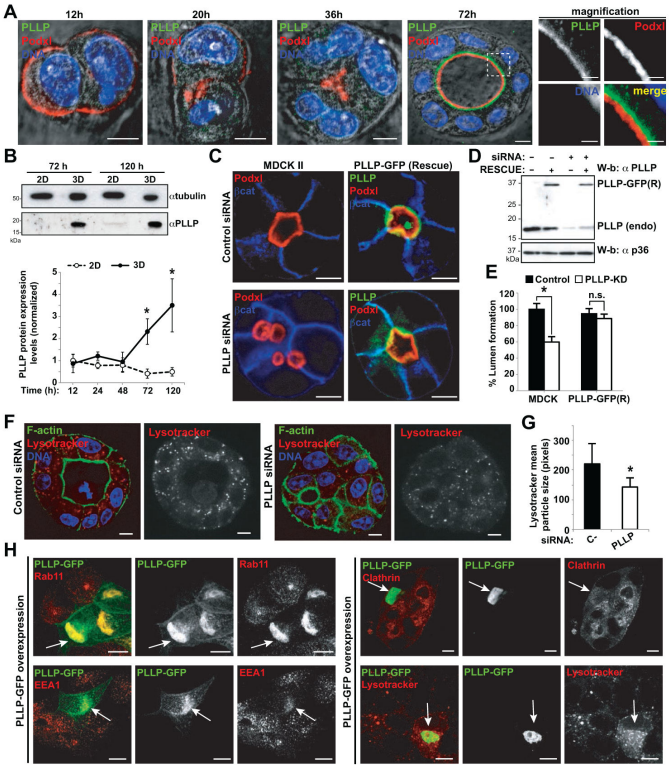

Figure 3. PLLP is required for epithelial morphogenesis and endosomal maturation in MDCK cysts

(A) Expression of PLLP in MDCK cysts at different time points. MDCK cells were grown to form cysts and fixed after 12, 20, 36 and 72h. MDCK cysts were labeled with anti-PLLP antibody (green), anti-Podxl (red), and DNA (blue) and analyzed by confocal microscopy using DIC. Scale, 5 μm (magnification, 2 μm).

(B) Expression of PLLP in MDCK cysts and monolayers at different time points. MDCK cells were grown to form cysts and lysed after 12, 24, 48, 72, and 120h. Western blot analysis was performed to quantify PLLP protein levels at different time points (bottom graph). Statistic source data can be found in Supplementary table 3.

(C) PLLP-KD phenotype in MDCK cysts, and phenotype rescue. WT MDCK cells or MDCK cells stably expressing siRNA-resistant PLLP-GFP(R) protein were transfected with control or PLLP-specific siRNAs and grown to form cysts. MDCK cysts were fixed and labeled with anti-Podxl (red) anti-βcatenin (blue) and analyzed by confocal microscopy. Scale, 5 μm.

(D) Western-blot of PLLP KD and rescue experiments. Whole cell lysates were prepared and analyzed by Western blot using anti-PLLP antibody and anti-p36 as a loading control.

(E) Quantification of PLLP-KD phenotype and rescue. Measurements are normalized to WT MDCK cells (control) and expressed as mean±SD percentage relative to control single lumen-forming cysts (Control, 100±7.2%, siRNA PLLP, 59.8±6.6%, PLLP(R)-control, 94.5±6.3%, PLLP(R)-siRNA PLLP, 88.7±5.4%; n=3 indendent transfection experiments; *p<0.005, n.s, not significant, Statistic source data can be found in Supplementary table 3).

(F) Endosomal acidification defect in PLLP-KD cysts. MDCK cells transfected with control or PLLP-specific siRNAs were grown to form cysts for 72h, labeled with Lysotracker-Red

for 2h, and then fixed. MDCK cysts were also labeled with Phalloidin (green) and ToPRO3 (DNA, blue) and analyzed by confocal microscopy. Scale, 5 μm.

(G) Quantification of endosomal acidification defect in (F). Data are represented as mean ±SD particle size in square-pixels (n=17 control and 18 PLLP-KD cysts selected randomly from 4 independent siRNA experiments; *$p<0.01$).

(H) Overexpression of PLLP-GFP in MDCK monolayers. MDCK cells transiently transfected with PLLP-GFP (green) were analyzed at 48h and labeled with anti-Rab11, anti-EEA1, anti-Clathrin and Lysotracker (red). Arrows indicate endosomal aggregates in PLLP overexpressing cells. Scale, 5 μm.

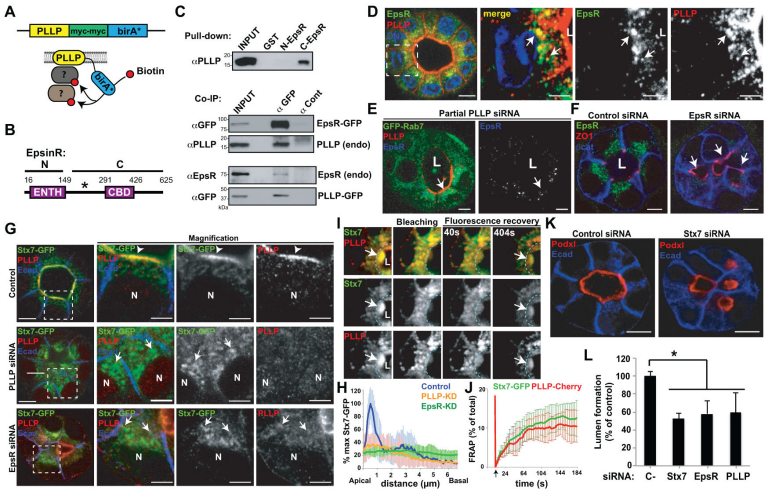

Figure 4. EpsR/PLLP mediate polarized apical sorting of endosomal SNARE Stx7

(A) *In vivo* biotinylation (bioID) assay to identify PLLP interacting proteins.

(B) Protein structure of EpsR. EpsR was biotinylated in a specific segment of the C-terminal region (asterisk).

(C) Pull down and coIP of endogenous PLLP and EpsR using GST-tagged EpsR fragments, EpsR-GFP or PLLP-GFP.

(D) Endogenous EpsR and PLLP localization. MDCK cysts were labeled with anti-PLLP antibody (red), anti-EpsR (green) and DNA (blue). Arrows indicate PLLP and EpsR colocalizing in perinuclear endosomes. Scale, 5 μm (magnification, 2 μm).

(E) Disrupted Rab7 and EpsR localization in PLLP-KD. MDCK cells stably expressing Rab7-GFP were transfected with PLLP siRNAs, grown in cysts and labeled with anti-PLLP (red) and anti-Epsin-R (blue). Arrow indicates non-depleted cells. Scale, 5 μm.

(F) Phenotype of EpsR-KD. MDCK cells were transfected with control or EpsR-specific siRNAs, grown in cysts and labeled with anti-EpsR (green), anti-ZO1 (red) and anti-βcatenin (blue). L, lumen. Arrows indicate multiple lumens. Scale , 5 μm.

(G) Stx7 localization in PLLP-KD and EpsR-KD MDCK cysts. MDCK cells stably expressing Stx7-GFP were transfected with control, PLLP, or EpsR-specific siRNAs, grown in cysts and labeled with anti-PLLP (red) and anti-E-cadherin (blue). Arrowheads indicate PLLP/Stx7 colocalization. Arrows indicate PLLP/Stx7 in perinuclear endosomes. Scale, 5 μm.

(H) Quantification of Stx7 localization in (G). GFP-Stx7 linear profiles were drawn perpendicular to the center of the apical plasma membrane. Data represented are averaged linear profiles ±SD (N>10 cells, n=3 different animals).

(I) Stx7 and PLLP FRAP assay. MDCK cells expressing PLLP-Cherry were transfected with Stx7-GFP and grown in cysts for 72h. Photobleaching was performed inside the region outlined by the dotted line, and cysts were imaged every 4 seconds. Scale, 5 μm.

(J) Quantification of FRAP assay. Data are mean±SD percentage of total fluorescence intensity inside the photobleached region. N=6.

(K) Phenotype of Stx7-KD. MDCK cells transfected with control or Stx7-specific siRNAs were grown in cysts and labeled with anti-Podxl (red) and anti-E-cadherin (blue). Scale, 5 μm.

(L) Quantification of phenotypes in PLLP-KD, EpsR-KD and Stx7-KD MDCK cysts. Measurements are expressed as mean±SD percentage (relative to control) of single lumen-forming cysts in 3 different independent experiments (control, 100±5.3%; Stx7-KD, 52.3±6.4%; EpsR-KD, 58.06±14.5%; PLLP-KD, 59.7±22.1%; n=3 independent transfection experiments; * $p<0.005$, Statistic source data can be found in Supplementary table 3).

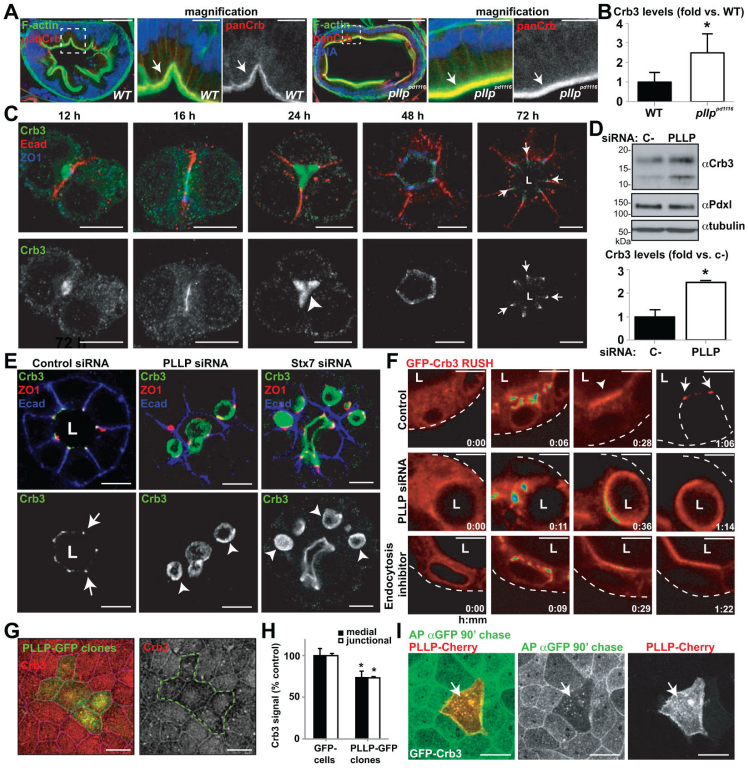

Figure 5. PLLP regulates Crb endocytosis

(A) Crb localization in WT and *pllp*^{pd1116} mutant 144hpf larvae. Sections were stained with anti-panCrb (red), Phalloidin (green) and DAPI (blue). Arrows indicate Crb localization at apical membrane. Scale, 20 μm (magnification, 10 μm).

(B) Quantification of Crb levels in (A). Data are represented as average fold-increase ±SD (WT, 1.00±0.50 fold; *pllp*^{pd1116}, 2.50±0.96 fold; n=6 wt and 6 mutant fish from 3 independent experiments; *p<0.005).

(C) Localization of endogenous Crb3. MDCK cysts were fixed and labeled with anti-Crb3 (green), anti-ZO-1 (blue) and anti-E-cadherin (red). Arrowhead indicates apical Crb3. Arrows indicate suprajunctional Crb3. Scale, 5 μm.

(D) Crb3 protein levels in PLLP-KD cysts. Data are expressed as mean±SD fold-increase vs. control (Control, 1±0.35 fold; PLLP-KD, 2.31±0.13 fold; n=3 extracts, *p<0.005, Statistic source data can be found in Supplementary table 3).

(E) Localization of endogenous Crb3 in PLLP-KD and Stx7-KD cysts. MDCK cells transfected with control, PLLP or Stx7-specific siRNAs, were grown in cysts and labeled with anti-Crb3 (green), anti-ZO-1 (red) and anti-E-cadherin (blue). L, lumen. Arrowheads indicate apical Crb3. Arrows indicate supra-junctional Crb3. Scale, 5 μm.

(F) Videomicroscopy of RUSH-Crb3a. RUSH-Crb3a MDCK cells were transfected with control or PLLP-siRNA and grown to form cysts. At 72h, biotin was added and cysts were recorded every minute until steady state. For endocytosis inhibition, cysts were treated with Dynasore after biotin addition. Arrowheads indicate apical membrane. Arrows indicate tight junctions. Dotted lines mark the basal contour of the cysts. L, lumen. Scale, 5 μm.

(G) Downmodulation of Crb3 in PLLP-GFP clones. PLLP-GFP transfected cells were grown as monolayers for 4 days mixed with control MDCK cells, fixed and labeled with anti-Crb3 (red). Dotted line indicates the PLLP-GFP expressing clone. Scale, 10 μm.
(H) Quantification of (G). Medial and junctional Crb3 staining was measured as mean % of control fluorescence intensity±SD (GFP-neg, 100±8.3%; PLLP-GFP, 73.6±7.7%; n=20 PLLP-GFP cells and 61 GFP-neg cells from 3 independent transfection experiments, *$p<0.01$).
(I) Pulse-chase endocytosis of GFP-Crb3a. MDCK cells stably expressing GFP-Crb3a were transfected with PLLP-Cherry. After 24h, the apical surface of the cells was incubated with anti-GFP to label Crb3 at 4ºC, washed, and cells were returned at 37º for 90 minutes. Then, cells were fixed and stained with anti-rabbit-Alexa647 (green). Images are maximum z-stack projections. Arrows indicate endocytosed apical GFP-Crb3a. Scale, 10 μm.

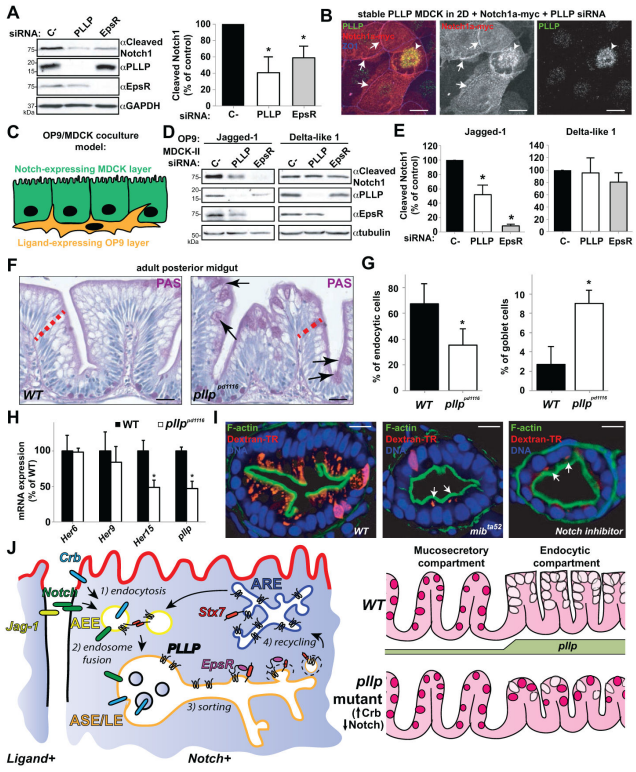

Figure 6. PLLP is required for Notch signaling

(A) Notch activation in PLLP-KD and EpsR-KD cysts. Cleaved Notch1 (NICD) protein levels were analyzed by Western blot. Data are mean±SD as % of control (PLLP, 41±19%, EpsR; 59±14%, n=3 extracts from 3 independent experiments, *p<0.05, Statistic source data can be found in Supplementary table 3).

(B) Notch localization in PLLP-KD cells. Cells were transfected with Notch1a-myc and PLLP siRNA and labeled with anti-myc (red), anti-PLLP (green) and anti-ZO1 (blue). Arrows indicate junctional Notch1a-myc in PLLP-depleted cells. Arrowheads indicate internal PLLP and Notch1a-myc colocalization in non-depleted cells. Scale, 10 μm.

(C) MDCK-II/OP9 coculture system for ligand-induced Notch1 transactivation assays.

(D) Effect of PLLP-KD or EpsR-KD on ligand-specific Notch1 transactivation. MDCK cells stably expressing Notch1a-myc were transfected with control, PLLP or EpsR-specific siRNAs and cultured with OP9 cells expressing Jagged-1 or Delta-like-1 and analyzed by Western blot.

(E) Quantification of Notch1 activity in (D). Data are mean±SD % of control cleaved Notch1 (PLLP-KD, 57.5±17.5%; EpsR-KD, 8.2±5.6%; n=3 extracts from 3 independent experiments, *p<0.05, Statistic source data can be found in Supplementary table 3).

(F) Intestinal morphology in adult *pllp*^{pd1116} posterior guts. Sections were stained with PAS (purple). Arrows indicate goblet cells. Red bars are placed to compare cell height. Scale, 20 μm.

(G) Quantification of endocytic cells and goblet cells. Data are expressed as mean±SD percentage of total cells from 9 crypts per animal (Endocytic cells: WT, 67.3±15.5%; *pllp*^{pd1116}, 35.3±12.4%; Goblet cells: WT, 2.7±1.8%; *pllp*^{pd1116}, 9.0±1.3%; n=6 wt, 6 mutant fish from 2 independent experiments; *p<0.005).

(H) Expression of Notch-target *hes-related* genes in WT and *pllp*^{pd1116} adult guts. Data are mean±SD percentage of control expression (n=3 extracts from 3 independent experiments; *p<0.01, Statistic source data can be found in Supplementary table 3).

(I) Dextran endocytosis in Notch-inhibited larvae. DMSO (control) or 100 μM DAPT (Notch inhibitor)-treated larvae and *mib1*^{ta52b} mutants were Dextran-gavaged (red) and stained with Phalloidin (green) and DNA (blue). Arrows indicate few remaining cells that are able to endocytose dextran. Scale, 10 μm.

(J) Model. Apical endosomal SNAREs, i.e. Stx7, are polarized. In mature sorting endosomes Pllp recruits EpsR, which binds Stx7 to recycle it specifically to the apical pole through the ARE. The patterned expression of Pllp in the zebrafish intestine regulates Crb and Notch receptor endocytosis and results in functional patterning of the midgut by promoting terminal differentiation of absorptive endocytic cells.